

Optimized design of next-generation multiplexing schemes for GNSSs

Original

Optimized design of next-generation multiplexing schemes for GNSSs / Nardin, Andrea; Dosis, Fabio; Perugia, Simone; Cristodaro, Calogero; Valle, Vittorio. - In: IET RADAR, SONAR & NAVIGATION. - ISSN 1751-8784. - ELETTRONICO. - 17:7(2023), pp. 1100-1104. [10.1049/rsn2.12403]

Availability:

This version is available at: 11583/2977312 since: 2023-05-05T16:16:07Z

Publisher:

Wiley

Published

DOI:10.1049/rsn2.12403

Terms of use:

This article is made available under terms and conditions as specified in the corresponding bibliographic description in the repository

Publisher copyright

IET preprint/submitted version (pre-accettazione)

This paper is a preprint of a paper submitted to IET RADAR, SONAR & NAVIGATION. If accepted, the copy of record will be available at the IET Digital Library

(Article begins on next page)

Optimized design of next-generation multiplexing schemes for GNSSs

Andrea Nardin,¹ Fabio Dovis,¹ Simone Perugia,² Calogero Cristodaro,² and Vittorio Valle²

¹Department of Electronics and Telecommunications, Politecnico di Torino, Turin, 10124, Italy

²Domain Observation and Navigation Italy (DONI), Thales Alenia Space Italy, Rome, 00131, Italy

Email: andrea.nardin@polito.it

Multilevel and multicarrier component signals are now common in many Global Navigation Satellite Systems challenging the employed multiplexing method that needs to be more flexible and powerful. In this work, we demonstrate how, by acting on two parameters of the digital baseband representation of component signals (the sampling frequency and the central frequency of the baseband complex envelope), it is possible to optimize the performance of the multiplexer, while still obtaining a composite signal that fulfills the required system constraints.

Introduction: Nowadays every Global Navigation Satellite System (GNSS) provides multiple positioning, navigation and timing (PNT) services to its users [1]. This diversified offer is ultimately enabled by the simultaneous broadcasting of several signals. However, the transmission of the resulting extended signal set needs to cope with the limited resource availability of a satellite's payload. In particular, it is desirable that the continuous transmission of different signals is performed throughout the same transmission chain (frequency up-converter, amplifier chain, and antenna) for the economical use of resources. The combination of these *component signals* into a *composite signal* over a shared medium is called *signal multiplexing*. Generally, in the satellite communications domain, the composite signal should exhibit a constant envelope (CE), to enable the high power amplifier (HPA) to operate at saturation, thus maximizing the power efficiency while preventing signal distortions. Besides CE, GNSS multiplexing methods should guarantee backward and forward compatibility to globally widespread receivers, that is they should be *transparent* to users [2]. Additionally, the necessary power loss employed to obtain a CE signal should be kept at its lowest, thus maximizing what is termed as the *multiplexing efficiency* [2–4].

PNT is made possible by GNSSs through the broadcasting of direct sequence spread spectrum (DSSS) signals. Traditionally they are composed of bipolar spreading chip waveforms transmitted over the same carrier, but in the last decades, the evolution of PNT services has brought in more complex waveforms. Multilevel spreading chips have been proposed to achieve better ranging accuracy [5]. On the other hand, the growing number of services have been also allocated to adjacent carriers [1] and the combination of these signals into a single composite multicarrier signal has become attractive to limit the number of amplifier chains [6] and to foster innovative receiver processing strategies [7, 8]. Nonetheless, the emerging low earth orbit (LEO) PNT paradigm [8–10] is encouraging a flexible PNT signals generation on payloads designed for rapid reconfiguration [9]. In such a framework, PNT services might be hosted on a telecommunication satellite, possibly sharing the existing payload and resources that are primarily dedicated to another service (e.g. internet broadband) [9]. In this variegated scenario, with signals becoming more complex and diverse, the need for highly-flexible and generalized signal multiplexing design has grown [4].

Multilevel and multicarrier waveforms are characterized by an increased number of possible values of amplitude and phase. This fact raises the complexity of the multiplexing algorithm which has to satisfy the aforementioned constraints (CE and transparency) for a large number of combinations of signal values while limiting the possible multiplexing efficiency reduction [2]. However, the number of signal value combinations—and more generally the multiplexer performance—are a consequence of the digital representation of the signal. The values taken by the digital samples when generated at baseband are strictly dependent on two parameters—the *central frequency* f_c with respect to which the baseband components are generated and the *sampling frequency* f_s —and both can be freely set to some extent, yielding an equivalent ana-

log Radio Frequency (RF) signal. Nonetheless, their choice impacts the complexity that the multiplexing algorithm has to face.

In this letter, we show how optimal f_c and f_s can improve the multiplexing efficiency with or without the knowledge of the multiplexing method. Specifically, these novel results show that these parameters have a large impact on variegated signal ensembles, promoting this flexible design approach to well-suit the needs of next-generation GNSSs and PNT services.

The Multiplexing Problem in GNSS: Let's consider a set of N orthogonal signal components $\tilde{s}_i(t)$ transmitted at several carrier frequencies $f_{i,\text{RF}}$. Ideally, the resulting RF signal should be

$$s_{\text{RF}}(t) = \sum_{i=1}^N \Re \{ \sqrt{P_i} e^{j\phi_i} \tilde{s}_i(t) e^{j2\pi f_{i,\text{RF}} t} \} \quad (1)$$

where P_i and ϕ_i are respectively the relative power and phase assigned to the i -th component by system design. A GNSS multiplexing scheme combines the $\tilde{s}_i(t)$ waveforms on both the in-phase and quadrature components of a single transmission chain, allowing to write the modulated signal as

$$s_{\text{RF,MUX}}(t) = \Re \{ s_{\text{MUX}}(t) e^{j2\pi f_{\text{RF}} t} \} \quad (2)$$

being $s_{\text{MUX}}(t)$ a complex envelope of the signal at f_{RF} , as depicted in Fig. 1. The modulated signal $s_{\text{RF,MUX}}(t)$ has a power spectral density (PSD) which retains the spectral properties of $s_{\text{MUX}}(t)$ shifted by f_{RF} . So to approach (1), the relative frequency separation among components should be preserved also in the baseband signal $s_{\text{MUX}}(t)$.

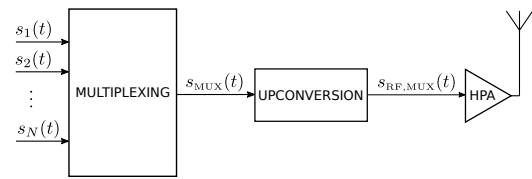


Fig 1 Multiplexer and high-level transmission chain.

In GNSS applications, the orthogonality of the components $\tilde{s}_i(t)$ allows the receiver to treat them separately through a correlation operation. Hence, a straightforward way to multiplex orthogonal signals is by direct superposition (DS), obtaining

$$s_{\text{DS}}(t) = \sum_{i=1}^N \sqrt{P_i} e^{j\phi_i} \tilde{s}_i(t) e^{j2\pi f_i t} \quad (3)$$

where we set

$$f_i = f_{i,\text{RF}} - f_{\text{RF}} \quad (4)$$

If $s_{\text{MUX}}(t) = s_{\text{DS}}(t)$ then $s_{\text{RF,MUX}}(t) = s_{\text{RF}}(t)$ is readily obtained through (2). More generally, $s_{\text{RF,MUX}}(t) \approx s_{\text{RF}}(t)$ as long as $s_{\text{MUX}}(t) \approx s_{\text{DS}}(t)$. However, for a generic set of signals $s_i(t) = \tilde{s}_i(t) e^{j2\pi f_i t}$ there are no obvious values for f_i . Indeed, while $f_{i,\text{RF}}$ is usually imposed by system design, f_{RF} can be freely set. In a digitized transmitter, for instance, we can assign $f_i = 0$ to an arbitrary i -th component, as long as its relative frequency separation with the other signals is maintained and the subsequent RF modulation is performed according to (4). We can write

$$f_{i,\text{RF}} = f_i + f_{\text{RF}} \quad (5)$$

$$= f_i - f_c + f_{\text{RF}} + f_c \quad (6)$$

$$= f'_i + f'_{\text{RF}} \quad (7)$$

and notice that the use of $f_i = f'_i$ in $s_i(t)$ would lead to a new composite signal $s_{\text{MUX}}(t)'$ represented with respect to a common frequency offset f_c . Nonetheless, the use of $f_{\text{RF}} = f'_{\text{RF}}$ would result in a modulated signal $s_{\text{RF,MUX}}(t)'$ which is also an approximation of (1), as illustrated by Fig. 2. From the signal generation perspective, there is no obvious choice of f_c .

To cope with the nonlinearity of the HPA, the multiplexer has to provide a signal $s_{\text{MUX}}(t) = A(t) e^{j\theta(t)}$ that after the upconversion to f_{RF} passes through the HPA with minimum distortions and power loss, i.e.

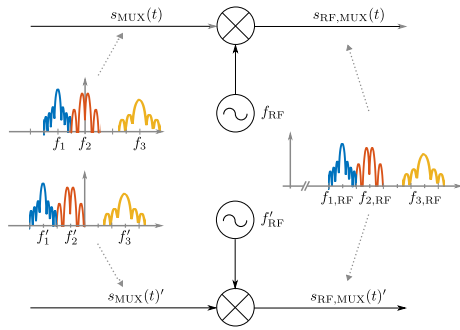


Fig 2 Equivalent frequency upconversion blocks.

a CE signal. To satisfy transparency, the orthogonality among the signal components has to be preserved, so that the component's power and phase can be recovered at the receiver side for every component i . This is done through a correlation operation whose output can be modeled as

$$R_i = \frac{1}{T_i} \int_{T_i} s_{MUX}(t) s_i(t)^* dt \approx \sqrt{P_i} e^{j\phi_i} \quad (8)$$

for some integration interval T_i . The approximation is motivated by generally non-perfectly orthogonal signals.

We can formalize the GNSS multiplexing problem as finding a mapping function $\Omega : \{s_1(t), \dots, s_N(t)\} \rightarrow s_{MUX}(t)$ subject to the conditions

$$\sqrt{P_i} e^{j\phi_i} = \frac{1}{T_i} \int_{T_i} s_{MUX}(t) s_i(t)^* dt \quad \forall i \quad (9)$$

$$s_{MUX}(t) = A e^{j\theta(t)} \quad (10)$$

Using DS would satisfy (9), but the envelope of $s_{DS}(t)$ is generally non constant. It is also desirable to maximize the multiplexing efficiency [3]

$$\eta = \frac{\sum_{i=1}^N |R_i|^2}{A^2} \quad (11)$$

Maximizing (11) means that the sum of the components' power measured at the correlator's output should be as close as possible to the power of the composite signal. The power gap between $s_{MUX}(t)$ and the sum of useful components corresponds to the power employed by the multiplexer to transform $s_{DS}(t)$ to a constant envelope signal. Such a relationship can be written as [2]

$$s_{MUX}(t) = s_{DS}(t) + s_{AUX}(t) \quad (12)$$

where $s_{AUX}(t)$ represents an auxiliary component. Note that not all the multiplexing algorithms explicitly compute $s_{AUX}(t)$, but the process can be described through (12) in the vast majority of cases [2].

Input optimization for multiplexing: In a digital implementation, a multilevel multicarrier signal component can be defined by

$$s_i[n] = \sum_{k=-\infty}^{+\infty} c_k^{(i)} p_i \left(\frac{n}{f_s} - k T_c^{(i)} \right) e^{j2\pi f_i \frac{n}{f_s}} \quad (13)$$

where $c_k^{(i)}$ is the k -th bipolar spreading symbol determined by the chip sequence and navigation data, and p_i is the pulse shape of the chip of duration $T_c^{(i)}$. It is clear from (13) that given a pulse shape for the i -th component, the set of possible values of $s_i[n]$ is determined by f_s and f_i . As multiple signal components are combined, the mapping Ω has to establish a relation between the value of the composite signal $s_{MUX}(t)$ and every different set of values that the signals in $\{s_1[n], \dots, s_N[n]\}$ can assume. Therefore, as the number and characteristics of these sets of combination values change, the complexity necessary to compute a feasible multiplexing mapping might increase. Thus, the resulting mapping has to satisfy (9) and (10), without disrupting the multiplexing efficiency performance. Indeed, f_s can be arbitrarily chosen, as long as the Nyquist limit is observed and possible additional constraints imposed by the hardware are respected. Similarly, the central frequency shift f_c with respect to which each f_i is defined can be freely set and the signal components can be generated through (13) updating f_i and f_{RF} in accordance with (6) and (7).

Given a set of signals, we can find the optimal baseband configuration that maximizes the multiplexing efficiency. In other words, we need to find

$$(\hat{f}_s, \hat{f}_c) = \arg \max_{f_s, f_c} \eta \quad (14)$$

The multiplexing efficiency is affected by f_s and f_c but is also determined by both the component signals waveforms and the multiplexing algorithm, which parametrize the function. A relationship that can be expressed through a function g so that

$$\eta = g(f_s, f_c; s_1[n], \dots, s_N[n], \Omega) \quad (15)$$

The complexity of multiplexing algorithms for multilevel and multi-carrier signals generally prevents the derivation of an explicit analytical expression for (15). Instead, the optimization must be done through exhaustive search, by exploring the whole solution space to identify the pair (f_s, f_c) that provides the best configuration for a given set of signal waveforms. This approach is computationally expensive since a mapping function Ω must be derived for each tested pair to compute $s_{MUX}(t)$ and the resulting η .

An alternative indicator of the multiplexing performance can be obtained from the original signal components alone. Indeed, the power loss spent to grant the constant envelope of $s_{MUX}(t)$, i.e. the power of $s_{AUX}(t)$, depends on how scattered the values of $|s_{DS}(t)|$ are, which is measured by the *nonconstancy* metric defined in [4]. Consider the *signal value vector* s_{DS} —a vector made of all the possible values assumed by $s_{DS}[n] = \sum_{i=1}^N \sqrt{P_i} e^{j\phi_i} s_i[n]$, sorted in ascending order. Such a vector contains an even number of elements for bipolar spreading symbols. A measure of the initial nonconstancy is given by

$$C = s_{DS}^H \mathbf{G} s_{DS} \quad (16)$$

where $\mathbf{G} = \text{diag}(-1 \dots -1 + 1 \dots +1)$ is a diagonal matrix whose first half of the diagonal contains a sequence of -1 and the second half is made of $+1$. It is easy to show that C is a nonnegative scalar function and $C = 0$ if and only if all the elements in $|s_{DS}|$ are equal. We can thus use (16) as a measure of how far a sum of signal components is from a constant envelope configuration. The initial lack of constancy does not depend on the multiplexing algorithm Ω , but it is still related to the resulting multiplexing efficiency. We can express its optimization as

$$(\hat{f}_s, \hat{f}_c) = \arg \min_{f_s, f_c} C \quad (17)$$

noting that

$$C = h(f_s, f_c; s_1[n], \dots, s_N[n]) \quad (18)$$

for an unknown function h that is not parametrized by Ω . Through this approach, we can eventually find the optimal f_s and f_c to get an initial set of signals whose sum is the closest to having a constant envelope. This will likely result in a composite signal with a high multiplexing efficiency, but the final result will ultimately depend on the mapping Ω (i.e. the multiplexing method). For this reason, C can be just an indicator of the multiplexing efficiency, but its independence from the adopted multiplexing scheme makes it a promising performance metric based solely on the signals' configuration.

Results and discussion: In this section, we analyze optimal f_s and f_c for a selected case study, i.e. a specific set of component signals and a multiplexing method. To provide timely and relevant results, we implemented the algorithm named CE multiplexing via intermodulation construction (CEMIC), a state-of-the-art multicarrier solution that achieves the highest multiplexing efficiency among existing methods [4]. A set of signal components has been chosen in line with modern GNSSs with some adaptations, trying to challenge both the multiplexer and the input optimization process. The signal characteristics and initial f_i values are summarized in Table 1 and the resulting PSDs are shown in Fig. 3. Notice that the signal $s_1[n]$ has been designed to maximize its Gabor bandwidth and increase its ranging accuracy [5] according to the well-known Cramér-Rao bound for time-delay estimation [1]. Its chip is defined by the sequence $p_1 = (-0.2, 0.375, -0.4, 0.5, -0.5, 0.4, -0.375, 0.2)$.

An exhaustive search of the best (f_s, f_c) pair in terms of multiplexing efficiency led to the results in Fig. 4. The search has been performed

Table 1. Component signals initial configuration.

Component	Modulation	Initial offset carrier ^a f_i	Phase	Power Ratio
s_1	MCS($[p_1]$,10) ^b	$-45f_0$	I	0.10
s_2	BPSK(10)	$-45f_0$	Q	0.15
s_3	BPSK(1)	0	I	0.10
s_4	BOC(10,5)	0	Q	0.30
s_5	CBOC(8,2,2/10)	$+30f_0$	I	0.35

^a Defined as multiple of $f_0 = 1.023$ MHz.

^b Multilevel coded spreading (MCS) [11].

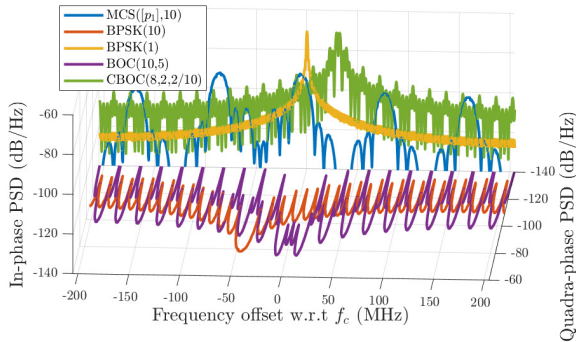


Fig 3 Component signals estimated PSD.

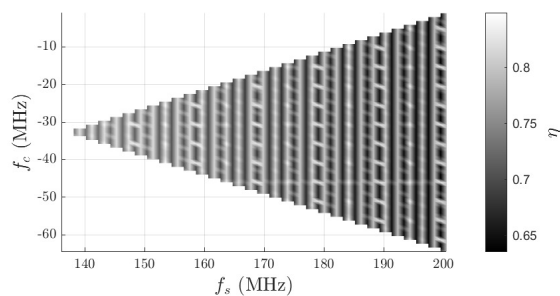


Fig 4 Multiplexing efficiency η w.r.t. f_s and f_c . Missing values are due to a resulting signal band sampled under the Nyquist limit.

with a step size of f_0 along both dimensions. Several configurations provide high multiplexing efficiency values, but the overall best is reported in Table 2 for the corresponding objective function. The nearly constant η values that can be found along the f_c direction in Fig. 4 suggest that some values of f_s negatively affect the multiplexing optimization process, regardless the chosen f_c . This could lead to a multiplexing efficiency power loss of up to 21.25%. Furthermore, as f_s increases, η exhibits generally lower values. Due to the presence of offset carriers, a high sampling frequency in (13) leads to a large number of possible signal values for which the multiplexing algorithm is less likely to be efficient in providing a CE signal.

We repeated the analysis over the same search space by assessing the initial constancy for each configuration. For this investigation, we built the signal value vector \mathbf{s}_{DS} to measure the nonconstancy through (16). The resulting values of C are shown in Fig. 5 and the corresponding optimal pair is reported in Table 2. The minimization of C led to the same (f_s, f_c) pair w.r.t. the previous experiment, corresponding to the same η value. Moreover, it can be noticed that the two plots of Fig. 4 and 5 exhibit a similar trend. Indeed, an analysis of the correlation among the computed values of η and C , performed through the Pearson correlation coefficient, showed that there is a correlation among these two variables of -0.99 for the case under study. This means that for a given signal components configuration when C is small there is a high chance that the multiplexing efficiency of the resulting signal $s_{MUX}(t)$ will be large and vice versa. The ultimate result depends on the chosen multiplexing method. However, it is reasonable to assume that a similar relationship holds for every multiplexing method as long as its mapping process can

Table 2. Component signals configuration.

Objective function	Optimal f_s	Optimal f_c	η
η	$150f_0$	$-30f_0$	0.848
C	$150f_0$	$-30f_0$	0.848

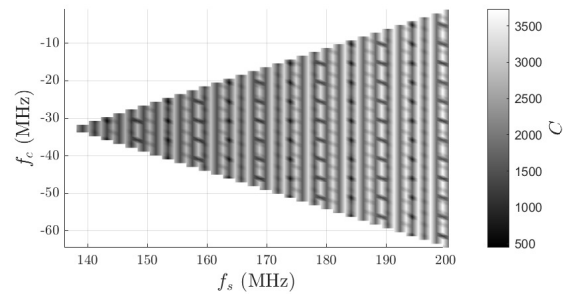


Fig 5 Nonconstancy C w.r.t. f_s and f_c .

be described by (12).

Conclusion: We saw that a bad choice of f_s and f_c can severely affect the multiplexing performance (Fig. 4) causing a power loss of more than 20%. Avoiding such poorly performing configurations motivates this input optimization analysis, which eventually provided non-trivial optimal solutions like the ones in Table 2. Moreover, a solution based on the overall constancy of the component signals configuration has been obtained. This solution is agnostic about the multiplexing method, having therefore a general significance, but is also not optimal in the multiplexing efficiency sense. Nonetheless, we found it to be an accurate indicator of the latter.

References

- Teunissen, P., Montenbruck, O.: Springer Handbook of Global Navigation Satellite Systems. vol. 4 of *Springer Handbooks*. 1st ed. Springer, Cham (2017)
- Yao, Z., Lu, M.: Signal multiplexing techniques for GNSS: The principle, progress, and challenges within a uniform framework. *IEEE Signal Processing Magazine* 34(5), 16–26 (2017)
- Dafesh, P.A., Cahn, C.R.: Phase-optimized constant-envelope transmission (POCET) modulation method for GNSS signals. In: *Proceedings of the 22nd International Technical Meeting of the Satellite Division of The Institute of Navigation (ION GNSS 2009)*, pp. 2860–2866. (2009)
- Yao, Z., et al.: Orthogonality-based generalized multicarrier constant envelope multiplexing for DSSS signals. *IEEE Transactions on Aerospace and Electronic Systems* 53(4), 1685–1698 (2017)
- Zhang, X., Yao, Z., Lu, M.: Optimizing the Gabor bandwidth of satellite navigation signals by MCS signal expression. *Science China Physics, Mechanics and Astronomy* 54(6), 1077–1082 (2011)
- Yao, Z., Lu, M.: Dual-frequency constant envelope multiplex with non-equal power allocation for GNSS. *Electronics Letters* 48, 1624–1625 (2012)
- Nardin, A., Dovis, F., Motella, B.: Impact of non-idealities on GNSS meta-signals processing. In: *2020 European Navigation Conference (ENC)*, , pp. 1–8. (2020)
- Nardin, A., Dovis, F., Fraire, J.A.: Empowering the tracking performance of LEO PNT by means of meta-signals. In: *2020 IEEE International Conference on Wireless for Space and Extreme Environments (WiSEE)*, , pp. 153–158. (2020)
- Iannucci, P.A., Humphreys, T.E.: Economical fused LEO GNSS. In: *2020 IEEE/ION Position, Location and Navigation Symposium (PLANS)*, , pp. 426–443. (2020)
- Nardin, A., Dovis, F., Fraire, J.A.: Empowering the tracking performance of LEO-based positioning by means of meta-signals. *IEEE Journal of Radio Frequency Identification* 5(3), 244–253 (2021)
- Rodríguez, J.Á.Á.: On Generalized Signal Waveforms for Satellite Navigation [dissertation]. Universität der Bundeswehr München (2008)